

## The angular momentum equation for a finite element of a fluid: A new representation and application to turbulent modeling

M. Iovieno and D. Tordella

Citation: *Phys. Fluids* **14**, 2673 (2002); doi: 10.1063/1.1485765

View online: <http://dx.doi.org/10.1063/1.1485765>

View Table of Contents: <http://pof.aip.org/resource/1/PHFLE6/v14/i8>

Published by the [American Institute of Physics](#).

---

### Related Articles

Inertial-range anisotropy in Rayleigh-Taylor turbulence  
*Phys. Fluids* **24**, 025101 (2012)

Modal versus nonmodal linear stability analysis of river dunes  
*Phys. Fluids* **23**, 104102 (2011)

The equivalence of the Lagrangian-averaged Navier-Stokes- $\alpha$  model and the rational large eddy simulation model in two dimensions  
*Phys. Fluids* **23**, 095105 (2011)

Amplification and nonlinear mechanisms in plane Couette flow  
*Phys. Fluids* **23**, 065108 (2011)

A shallow water model for magnetohydrodynamic flows with turbulent Hartmann layers  
*Phys. Fluids* **23**, 055108 (2011)

---

### Additional information on Phys. Fluids

Journal Homepage: <http://pof.aip.org/>

Journal Information: [http://pof.aip.org/about/about\\_the\\_journal](http://pof.aip.org/about/about_the_journal)

Top downloads: [http://pof.aip.org/features/most\\_downloaded](http://pof.aip.org/features/most_downloaded)

Information for Authors: <http://pof.aip.org/authors>

### ADVERTISEMENT



**Running in Circles Looking  
for the Best Science Job?**

Search hundreds of exciting  
new jobs each month!

<http://careers.physicstoday.org/jobs>

physicstodayJOBS



# The angular momentum equation for a finite element of a fluid: A new representation and application to turbulent modeling

M. Iovieno and D. Tordella

*Dipartimento di Ingegneria Aeronautica e Spaziale, Politecnico di Torino, C.so Duca degli Abruzzi 24, 10129 Torino, Italy*

(Received 7 February 2001; accepted 24 April 2002; published 20 June 2002)

The equation for the intrinsic moment of momentum averaged over small volumes of linear dimension  $\delta$  has been considered. A representation of it is given as an infinite sequence of independent equations using a series expansion in terms of  $\delta^2$ . The equations of different orders are obtained through linear antisymmetric operators—with a structure that is similar to that of the curl—acting on the momentum equation. The first-order term of the sequence is the Helmholtz equation; the remaining terms can be considered as balances for a kind of higher-order vorticity. It has been shown that the coupling between the momentum and the angular momentum equation, based on a supposed antisymmetrical part of the stress tensor—which has sometimes been assumed by authors who deal with turbulent flow of a homogeneous fluid—is devoid of physical rationale. A different form of coupling is proposed that may be used to describe a turbulent flow of a homogeneous medium, using a large eddy simulation technique. In the authors model the coupling is given by a functional dependence of the turbulent eddy diffusivity over the angular momentum of a finite volume of a fluid. © 2002 American Institute of Physics. [DOI: 10.1063/1.1485765]

## I. INTRODUCTION

To deal with a nonhomogeneous fluid with internal structures on which external forces and couples act, it is necessary to introduce a balance of angular momentum, whose presence affects the symmetry property of the stress tensor.<sup>1–5</sup> In this case the moment of the momentum equation is no longer equivalent to the angular momentum budget and a new variable, the intrinsic angular momentum per unit volume, must necessarily be introduced.

The micropolar theory<sup>6–8</sup> views the medium as a collection of material systems, the microelements, containing momentum, intrinsic angular momentum, and energy. The microelements can contain internal structures (like liquid crystals, blood cells,...), however, the fluid is viewed as monophasic. The motion of the microelement is fully described by the velocity of its centroid and by a second-order tensor—called the microgyration tensor—which portrays the internal deformation and rotation of the element. The centroid velocity and the microgyration tensor vary continuously in the external scale of the field. In an incompressible flow, Eringen's theory leads to a set of 12 differential equations, from which the intrinsic moment of momentum can be recovered by taking the antisymmetrical part of the microgyration tensor. The equation of the intrinsic angular momentum appears to be coupled to the momentum equation expressed in terms of the centroid velocity in such a way as to establish a link between the intrinsic motion inside the microelements and the mean velocity field.

The equation of angular momentum balance has been applied a few times during the last century to discuss the behavior of turbulent flows. Since the earliest application in 1933 by Mattioli, the equations of motion were often integrated over finite volumes to show the evolution of the large

scales of the turbulence. Even with fluids deprived of internal structures, asymmetry was associated to the turbulent stress in Mattioli<sup>9,10</sup> and in Nicolaevsky.<sup>11,12</sup> In Eringen,<sup>13</sup> the micropolar theory was applied to turbulence.

In Sec. II an analysis was carried out on the structure of the angular momentum budget over finite volumes of linear dimension  $\delta$ . The analysis is relevant to all situations where the fluid may be considered locally homogeneous. Through a power series development in the square of the linear dimension of average we show that the balance for the intrinsic momentum may be represented by an infinite succession of independent equations obtained by applying linear antisymmetric operators to the momentum balance. The first-order term of the sequence is the vorticity equation,<sup>14,15</sup> while the higher-order relations are not reducible to it and may be viewed as high-order vorticity budgets.

Applications of theories relevant to structured flows to turbulence are discussed in Sec. III A through an analysis of the symmetry property of the Navier–Stokes equations. The common aspects of these theories and their physical support are discussed. In Sec. III B, in the ambit of turbulence modeling, a different kind of coupling is suggested between the momentum and angular momentum turbulent equations, which does not rely on the supposed existence of the antisymmetric part of the stress tensor. A large eddy scale model that is based on the proportionality of the turbulent diffusivity to the intrinsic moment of momentum is proposed here. The principal features of this model are the correct scaling of the eddy diffusivity  $\nu_\delta$ , with respect to both the filtering length  $\delta$  and the dissipation rate function, and the introduction of a differential equation—the intrinsic angular momentum equation—to follow the evolution of  $\nu_\delta$ . This equation introduction should be advantageous in the case of simulation of nonequilibrium turbulence fields, since it adds a de-

gree of freedom to the model. A natural application for this model would be the turbulent motion of suspensions of massive particles on which external couples apply, such as, for example, a dusty plasma flow. In such a case the model would no longer be differential since the coupling between the momentum and the angular momentum equations is already present and associated to the physics of the problem. The model validation is described in Sec. III C.

## II. ANGULAR MOMENTUM AND VORTICITY IN MONOPHASE FLOWS

The relationship between angular momentum and vorticity and between their equations is considered here. It is usually assumed that vorticity represents the angular velocity of a small volume of fluid. The vorticity equation is obtained by considering the curl of the momentum equation. Working on volume-averaged equations, at a first-order approximation of the angular momentum expanded in the square of the linear dimension of average  $\delta$ , Nigmatulin and Nikolaevsky,<sup>15</sup> for an incompressible flow, and Chatwin,<sup>14</sup> for a barotropic flow, showed the proportionality of vorticity to the angular momentum.

Here we have expanded the intrinsic angular momentum in the neighborhood of a point  $\mathbf{x}$  by means of a power series in  $\delta$ . The expansion is carried out at the general order  $n$ . As a result, an infinite sequence of independent linear antisymmetric differential operators, the first of which is the curl, is obtained. Applying the operators to the momentum balance, a correspondent infinite sequence of independent equations is also obtained, where the first-order term is the Helmholtz equation.

In the neighborhood of a point  $\mathbf{x}$ ,

$$\mathcal{I}_\delta = \{\mathbf{x} + \boldsymbol{\eta} \in \mathbb{R}^3 : \|\boldsymbol{\eta}\| < \delta\},$$

the spatial average operator  $\langle \cdot \rangle_\delta$ ,

$$\langle \varphi \rangle_\delta(\mathbf{x}, t) = \frac{1}{V_\delta} \int_{\mathcal{I}_\delta} \varphi(\mathbf{x} + \boldsymbol{\eta}, t) d\boldsymbol{\eta}, \quad (1)$$

has been introduced, where  $\delta$  is the linear dimension of  $V_\delta$ , which is the volume of  $\mathcal{I}_\delta$ . To simplify the notation, suffix  $\delta$  will be usually omitted in the following. The intrinsic moment operator  $\mathbf{M}$  acting on a vector field  $\mathbf{f}$  is defined as

$$(\mathbf{M}\mathbf{f})_i = \varepsilon_{ijk} (\langle x_j f_k \rangle - \langle x_j \rangle \langle f_k \rangle). \quad (2)$$

Expanding  $\mathbf{f}$  in the neighborhood of  $\mathbf{x}$ , we obtain

$$(\mathbf{M}\mathbf{f})_i = \varepsilon_{ijk} \sum_{t=0}^{\infty} \sum_{s=0}^t \sum_{r=0}^s \frac{1}{t!} \binom{t}{s} \binom{s}{r} \times \partial_j^r \partial_p^{s-r} \partial_q^{t-s} f_k \left( \frac{1}{V_\delta} \int_{\mathcal{I}_\delta} \eta_j^{r+1} \eta_p^{s-r} \eta_q^{t-s} d\boldsymbol{\eta} \right), \quad (3)$$

where  $j, p$ , and  $q$  are clockwise permutations of 1, 2, and 3. The transformation  $\boldsymbol{\eta} = \delta \boldsymbol{\zeta}$  shows the dependence on the powers of  $\delta$ ,

$$\begin{aligned} & \frac{1}{V_\delta} \int_{\mathcal{I}_\delta} \eta_j^{r+1} \eta_p^{s-r} \eta_q^{t-s} d\boldsymbol{\eta} \\ &= \left( \frac{1}{V_1} \int_{\mathcal{I}_1} \zeta_j^{r+1} \zeta_p^{s-r} \zeta_q^{t-s} d\boldsymbol{\zeta} \right) \delta^{r+1}. \end{aligned} \quad (4)$$

Due to the symmetry property of  $\mathcal{I}_\delta$ , the nonzero integrals in (4) are those for which  $t, s$ , and  $r$  are all odd. Placing  $t = 2n + 1, s = 2m + 1, r = 2\ell + 1$  we define the coefficients

$$a^{n,m,\ell} = \frac{1}{V_1} \int_{\mathcal{I}_1} \zeta_j^{2(\ell+1)} \zeta_p^{2(m-\ell)} \zeta_q^{2(n-m)} d\boldsymbol{\zeta}, \quad (5)$$

which represent the moments of the average volume of unit radius. Due to the symmetry of the average volume, these coefficients do not depend on the permutations  $j, p$ , and  $q$ .

In such a way the operator  $\mathbf{M}$  is expanded in a series of power of  $\delta^2$ :

$$\mathbf{M} = \sum_{n=0}^{\infty} \frac{\delta^{2n+2}}{(2n+1)!} \mathbf{A}^{(n)}, \quad (6)$$

where

$$\begin{aligned} A_{ik}^{(n)} &= \varepsilon_{ijk} \sum_{m=0}^n \sum_{\ell=0}^m \binom{2n+1}{2m+1} \binom{2m+1}{2\ell+1} \\ &\times a^{n,m,\ell} \partial_j^{2\ell+1} \partial_p^{2(m-\ell)} \partial_q^{2(n-m)}. \end{aligned}$$

The mean intrinsic angular momentum per unit mass  $\mathbf{h}$  of each element  $\mathcal{I}_\delta$  is defined as

$$\langle \rho \rangle \mathbf{h} = \mathbf{M}(\rho \mathbf{u}). \quad (7)$$

From (6), and similar expansions of the averaged density, e.g.,

$$\langle \rho \rangle^{-1} = \rho^{-1} \left( 1 - a^{0,0,0} \nabla^2 \rho \frac{\delta^2}{2} + O(\delta^4) \right),$$

truncated expansions for the intrinsic angular momentum can be obtained. For instance, the expansion of the fourth order is

$$\begin{aligned} h_i &= a^{0,0,0} \varepsilon_{ijk} \frac{\partial_j(\rho u_k)}{\rho} \delta^2 + \frac{1}{\rho} \left( -\frac{1}{2} (a^{0,0,0})^2 \varepsilon_{ijk} \partial_j(\rho u_k) \frac{\nabla^2 \rho}{\rho} \right. \\ &+ \frac{1}{3!} [3a^{1,0,0} \nabla^2 \varepsilon_{ijk} \partial_j(\rho u_k) \\ &+ (a^{1,1,1} - 3a^{1,0,0}) \varepsilon_{ijk} \partial_j^3(\rho u_k)] \left. \right) \delta^4 + O(\delta^6). \end{aligned} \quad (8)$$

The operator  $\mathbf{M}$  applied to the momentum equation,

$$f_k(\mathbf{x}, t) \equiv \partial_t(\rho u_k) + \partial_\ell(\rho u_k u_\ell) - \partial_\ell \sigma_{k\ell} - \rho b_k = 0,$$

where  $\boldsymbol{\sigma}$  is the stress tensor and  $\mathbf{b}$  is an external force field, yields the budget for  $\mathbf{h}$  in terms of a series expansion in  $\delta^2$ . Since this equation is an identity in  $\delta$ , the coefficient of each  $\delta^{2(n+1)}$  must vanish independently; that is,  $\mathbf{A}^{(n)} \mathbf{f} = \mathbf{0}, \forall n \in \mathbb{N}$ , which reduces to

$$\varepsilon_{ijk} \partial_j^{2n+1} f_k(\mathbf{x}, t) = 0, \quad \forall n \in \mathbb{N}, \quad i, j, k = 1, 2, 3,$$

as can be shown by induction. Free of any approximation, the angular momentum budget leads to a sequence of differential equations that cannot be reduced to each other, the leading order of which is the vorticity equation. Thus,  $\mathbf{h}$  cannot be described in terms of only vorticity  $\boldsymbol{\omega}$ . Only when  $\delta \rightarrow 0$ ,  $\mathbf{h}$  does contain the same amount of information as  $\boldsymbol{\omega}$ , but in this case  $\boldsymbol{\omega}$  goes to zero as  $\delta^2$ .

The higher-order equations of the sequence may be interpreted as balances for high-order vorticities. The result is quite general because it is not restricted by the particular nature of the constitutive equation, as long as the latter describes a fluid—even though with internal structures—as a fluid with bulk properties. The higher-order terms of this sequence may become useful in turbulence applications, where auxiliary-independent equations are required for the correlation variables that are introduced by the filtering process.

### III. ANGULAR MOMENTUM AND TURBULENCE

#### A. Applications to turbulence of structured fluid theories

In Eringen,<sup>13</sup> the microfluid theory, that was conceived for structured fluids, was applied to a turbulent flow of a nonstructured fluid. Analogous approaches were proposed in the past by Mattioli<sup>9,10</sup> and Ferrari,<sup>16</sup> where an intrinsic angular momentum was introduced to represent the turbulent transport, and by Nikolaevsky,<sup>11,12</sup> who approximated the volume average of the spatial derivatives in terms of an incremental ratio of surface integrals thus introducing asymmetry into the turbulent stress.

The crucial point of these theories is the coupling between the momentum and the moment of momentum equations. In all these theories the distribution of the mean velocities depends on the motion of internal rotation, which is considered as the structural property of the elemental cells, the so-called microelements. The mathematical coupling between the two kinematical aspects is due to the presence of the antisymmetrical part of the stress tensor in both momentum and angular momentum equations.

This aspect is explicitly declared in Mattioli and it has been renewed by Ferrari and Nicolaevsky, but is also a necessary element in the model by Eringen. All these theories seem capable of reproducing experimental results concerning turbulent sheared flows. In spite of this, their common and decisive component—the coupling between the momentum and angular momentum equations through an antisymmetrical part of the stress tensor—is an arbitrary choice, whose validity in the case of a homogenous fluid can be proved false.

The volume average for a function  $f$ , already introduced in Sec. II, may be written as

$$\langle f \rangle(\mathbf{x}) = \int_{R^3} g_\delta(\mathbf{x}-\mathbf{y})f(\mathbf{y})d\mathbf{y} = \int_{R^3} g_\delta(\mathbf{y})f(\mathbf{x}-\mathbf{y})d\mathbf{y}, \quad (9)$$

where  $f$  and  $g_\delta \in L^1$ , together with their derivatives. Function  $g_\delta$  is the weight function that shapes the space portion where the average is taken. Under these assumption, the first spatial derivative and the volume average commute:

$$\begin{aligned} \langle \partial_i f \rangle(\mathbf{x}) &= \int_{R^3} g_\delta(\mathbf{y})\partial_i f(\mathbf{x}-\mathbf{y})d\mathbf{y} \\ &= \int_{R^3} \partial_i [g_\delta(\mathbf{y})f(\mathbf{x}-\mathbf{y})]d\mathbf{y} = \partial_i \langle f \rangle. \end{aligned} \quad (10)$$

Relation (10) implies that this spatial filtering is unable to break the symmetry property of flow tensors, independently of the kind of regime of motion, whether laminar or turbulent. To verify this inference, it is sufficient to apply the filtering to the Navier–Stokes equations that, in case of incompressible flow, yields

$$\begin{aligned} \rho D_t \langle u_i \rangle &= \partial_j [ - \langle p \delta_{ij} \rangle + \mu (\partial_j \langle u_i \rangle + \partial_i \langle u_j \rangle) \\ &\quad + \rho (\langle u_i \rangle \langle u_j \rangle - \langle u_i u_j \rangle)]. \end{aligned} \quad (11)$$

The theories by Mattioli, Ferrari, and Nikolaevsky adopt the following structure for incompressible turbulence equations of a homogeneous fluid:

$$\rho D_t \langle u_i \rangle = \partial_j \sigma_{ij} + \partial_j \tau_{ij}^a + \partial_j \tau_{ij}^s, \quad (12)$$

$$\rho D_t h_i = \varepsilon_{ijk} \tau_{jk}^a + \partial_j c_{ij} + \partial_j s_{ij}, \quad (13)$$

where superscripts  $a$  and  $s$  stand for antisymmetric and symmetric and all the tensors are volume-averaged quantities:  $\sigma_{ij}$  and  $\tau_{ij}$  are the molecular and turbulent stress tensors, while  $s_{ij}$ ,  $c_{ij}$  are the molecular and turbulent flow tensors of angular momentum, respectively. There is no doubt that the averaged velocity indicates the same variable in Eqs. (11) and (12) and thus that the equations cannot both be true.

In Mattioli's theory the antisymmetrical part of the turbulent stress is assumed and interpreted as the momentum transport due to the vortical structures of the small scales that are filtered from the equation. A model is therefore required for this term. He also assumed, though not quite legitimately, since he dedicated an evolutive equation to it, that the intrinsic moment is proportional to the vorticity. The angular momentum budget thus becomes an equation that operates on the vorticity. This budget has, however, a different structure from the original Helmholtz equation because of the presence of the term  $\varepsilon_{ijk} \tau_{jk}^a$ . In this manner one dependent variable is dropped. The balance is then used to model the turbulent transport coefficient. Contrary, to what has been done for the momentum, the inertial tensor  $c_{ij}$  is assumed symmetric.

Nikolaevskij,<sup>11</sup> while computing (9) over cubes, introduces an approximation of the second order in  $\delta$  that induces the lost of property (10) and thus of the property of symmetry of the averaged equation, inside which he obtains the divergence of asymmetrical tensors. He, in fact, uses the Gauss theorem to transform the integral of the divergence into a surface integral. He then he approximates derivatives with the incremental ratios:

$$\left\langle \frac{\partial f}{\partial x_i} \right\rangle = \frac{\partial}{\partial x_i} [f]_{(i)} + O(\delta^2),$$

where one should not sum over the index in parentheses and  $[f]_{(i)}$  is defined by

$$[f]_{(i)} = (2\delta)^{-2} \int_{-\delta}^{\delta} \int_{-\delta}^{\delta} f(\mathbf{x} + \eta_j \mathbf{e}_j + \eta_k \mathbf{e}_k) d\eta_j d\eta_k.$$

Nikolaevskij neglects the terms  $O(\delta^2)$ . In so doing, he loses the symmetry of the tensors involved in the equations, together with the commutability.

In the application of the microfluid theory to turbulence, by Eringen,<sup>15</sup> the turbulent flow is considered as the motion of a simple microfluid, even though any physical internal structure that could cause asymmetry is missing.

The motion of the micropolar element is described by the mean velocity  $v_k(\mathbf{x}, t)$  and by the microgyration tensor  $\nu_{kl}(\mathbf{x}, t)$  ( $k, l = 1, 2, 3$ ). The latter arises from the motion and deformations of material points inside the volume of the microelement. The resulting system of equations—which are not reducible to the filtered Navier–Stokes equations—comprehends 12 scalar equations for the three components of the mean velocity and for the nine components of  $\nu_{kl}(\mathbf{x}, t)$  and contains 23 constant viscosity coefficients. The intrinsic moment of the momentum equation, which can be obtained from the antisymmetrical part of  $\nu_{kl}(\mathbf{x}, t)$ , is coupled to the momentum equation through the antisymmetrical part of the stress tensor, as in Mattioli and Nikolaevsky. In his solution for the two-dimensional (2-D) turbulent channel flow, Eringen gives a solution of his system of equations where the stress tensor is nonsymmetric. The constant coefficients, which are only five thanks to the simple domain geometry, were adjusted according to the experimental observations by Laufer.<sup>17</sup> However, it is easily seen that if the nonsymmetric part of the stress tensor is placed equal to zero, the equations result to be uncoupled and the mean motion would be independent of the internal motion of the microelements.

**B. Angular momentum large eddy model for turbulent flows**

In this paragraph we would like to propose a different kind of coupling of the momentum and angular momentum equations, which does not require that a nonsymmetry part of the stress tensor exists. In the framework of the large eddy scale simulation, a new differential model is proposed for the turbulent stresses that is based on a Boussinesq transport coefficient that is proportional to the mean intrinsic moment modulus  $h$ , a flow integral quantity that takes into account velocity derivatives of any odd order [see Sec. II, Eqs. (6) and (7)], and that is supposed to include both the mechanisms of stretching and the process of autodiffusion. The coupling between the momentum and moment of momentum equations is thus given by the functional dependence of the eddy diffusivity over the intrinsic angular momentum of a finite volume of a fluid. Let us consider the incompressible momentum equation,

$$\partial_t(u_k) + \partial_l(u_k u_l) = \frac{1}{\rho} \partial_l \sigma_{kl} + b_k,$$

where  $\sigma_{kl}$ ,  $b_k$  are the stress tensor and the external field, respectively. Applying the average operator  $\langle \cdot \rangle_{\delta}$ , the momentum equation is written in the following form:

$$D_t \langle u_i \rangle = \rho^{-1} \partial_j \langle \sigma_{ij} \rangle + \partial_j \tau_{ij} + \langle b_i \rangle, \tag{14}$$

where  $\tau_{ij} = \langle u_i \rangle \langle u_j \rangle - \langle u_i u_j \rangle$  is the turbulent momentum flow per unit mass. The intrinsic angular momentum equation is obtained by applying the operator  $\mathbf{M}$  [relation (2) in Sec. II] to the incompressible Navier–Stokes equation. The addition of the term  $\varepsilon_{i/k} [(\langle x_l u_k \rangle - \langle x_l \rangle \langle u_k \rangle) \langle u_j \rangle - (\langle x_l u_k u_j \rangle - \langle x_l \rangle \langle u_k u_j \rangle)]$ —the convection of the intrinsic angular momentum per unit mass by means of the averaged velocity field—to each side of the resulting balance yields the following equation for  $h_i$ , that is, the intrinsic angular momentum per unit mass of the element  $\mathcal{I}_{\delta}$  [see (7), Sec. II]:

$$D_t h_i = \rho^{-1} \partial_j s_{ij} + \partial_j c_{ij} + \beta_i, \tag{15}$$

where

$$c_{ij} = \varepsilon_{i/k} [(\langle x_l u_k \rangle - \langle x_l \rangle \langle u_k \rangle) \langle u_j \rangle - (\langle x_l u_k u_j \rangle - \langle x_l \rangle \langle u_k u_j \rangle)], \tag{16}$$

$$s_{ij} = \varepsilon_{i/k} (\langle x_l \sigma_{kj} \rangle - \langle x_l \rangle \langle \sigma_{kj} \rangle), \tag{17}$$

$$\beta_i = \varepsilon_{i/k} (\langle x_l b_k \rangle - \langle x_l \rangle \langle b_k \rangle), \tag{18}$$

are, respectively, the inertial (containing stretching) and interaction flow tensors of angular momentum and  $\beta$  is the couple associated to the external field  $\mathbf{b}$ .

The terms inside Eqs. (14) and (15) that need to be represented through a model are the turbulent momentum and angular momentum stresses. The functional relations on which the model relies are all Galilean invariants and are listed below:

$$\nu_{\delta} = ch, \tag{19}$$

$$\tau_{ij} = ch(\partial_j \langle u_i \rangle + \partial_i \langle u_j \rangle - \frac{2}{3} \partial_k \langle u_k \rangle \delta_{ij}), \tag{20}$$

$$c_{ij} = \langle u_i \rangle h_j + ch(\partial_j h_i + \partial_i h_j - \frac{2}{3} \partial_k h_k \delta_{ij}), \tag{21}$$

where  $c$  is a subgrid constant.

The first term on the right-hand side of (21) represents the role played by the stretching, while the other simulates the momentum transfer due to the turbulent convection. The present day reference large eddy simulation method is based on the adoption of Smagorinsky’s<sup>18</sup> or the vorticity<sup>19</sup> models, which assume a local invariance of the turbulent motion. Thus, in the immediate vicinity of a point, in time and space, a dynamical similarity is assumed throughout the field. The nondimensionalization of the field is based on the existence of local turbulent scales that are small enough to adjust to the slowly changing environment in the external scale. With this model one degree of freedom is introduced—the intrinsic angular momentum—which is portrayed by a relevant differential equation, which is coupled but, however, independent of the momentum equation. In this way we also hope to be able to simulate a turbulent flow that is not in local equilibrium. This would, of course, depend on the propriety with which the turbulent flow tensor of the intrinsic moment of momentum is modeled. In relation (21) it was attempted to insert the two major inertial phenomena that are present at the level of the subgrid scales, the stretching and the transport due to the turbulent convection.

In spite of the introduction of an additional differential equation, only one subgrid constant  $c$  appears in the model.

Assuming that the largest resolvable wave number lies within the inertial range, that the energy transferred from the resolved scales to the subgrid scales is equal to the energy dissipated by the latter and that the energy of the subgrid scales is that contained by their inertial part (see Lilly<sup>20</sup> and Yoshizawa<sup>21</sup>) constant  $c$  may be estimated as 0.066 (see Appendix A for details).

Note that in local turbulence equilibrium conditions the scaling of the turbulent viscosity, with respect to the dissipation function  $\epsilon$  and the filtering length  $\delta$ , is the same as that of the intrinsic angular momentum,

$$h \sim \delta^{4/3} \epsilon^{1/3} \sim \nu_\delta. \tag{22}$$

For the derivation of these scaling laws see Monin and Yaglom<sup>22</sup> as regards  $h$  and Yoshizawa,<sup>21</sup> Leslie and Quarini<sup>23</sup> as regards  $\nu_\delta$ .

As a comment on the functional structure of the present model, it is possible to draw a parallel between the latter and the mixed subgrid model (Bardina *et al.*, 1980):<sup>24</sup>

$$\tau_{ij}^{\text{mix}} = c_{\text{sim}}(\langle\langle u_i \rangle\rangle \langle\langle u_j \rangle\rangle - \langle\langle u_i \rangle \langle u_j \rangle \rangle) + 2(c_s \delta)^2 |\langle D \rangle| \langle D_{ij} \rangle,$$

where  $c_{\text{sim}}$  and  $c_s$  are the similarity and Smagorinsky subgrid coefficients and  $D_{ij}$  is the strain rate tensor. The analogy consists in the fact that the first terms of the expansions in series of  $\delta$  of the similarity subgrid tensor  $\tau_{ij}^{\text{sim}}$  and of the real subgrid tensor ( $\tau_{ij} = \langle u_i \rangle \langle u_j \rangle - \langle u_i u_j \rangle$ ) are both proportional to  $\partial_m u_i \partial_m u_j \delta^2$ , while the first terms of the expansions in series of  $\delta$  of relation (21) and of the inertial tensor of the flow of intrinsic angular momentum (16) are both proportional to  $u_i \omega_j \delta^2$  (see Appendix B for details). From this aspect we can infer that the present model could feature a certain degree of backscatter: directly on  $h_i$  and indirectly on  $\nu_\delta$ . Also of interest is the fact that—in the context of spectral numerical simulations—the number of spectral products that are necessary to implement the angular momentum model, in spite of the fact that it is a differential model, is exactly the same as the number of spectral products that are necessary to implement the mixed model.

In short, the main features of this model are the following: the capability of following the evolution of  $h$ , and thus of  $\nu_\delta$ , through a relevant differential equation and the proper scaling with respect to the filtering length and the dissipation rate. The differential nature would suggest an employment of nonequilibrium turbulent flows for simulations.

A unique feature of the present model is its natural convenience to simulate the dynamics of structured fluid in turbulent motion. In this case, the coupling between the momentum and angular momentum equations already having been introduced by the physics of the system, the model reduces from differential to algebraic.

### C. Numerical validation of the angular momentum large eddy model

The results obtained from tests concerning the statistical and spectral properties of (i) homogeneous and isotropic tur-

bulence, (ii) homogeneous turbulence undergoing a solid body rotation, and (iii) shear-free nonhomogeneous turbulence are presented in this section.

Before beginning the discussion on the numerical tests, the criteria adopted to carry out the comparison of the angular momentum model in the simplest way with different subgrid models are described—the Smagorinsky and the mixed models—being chosen as reference. Since an optimized value for the angular momentum model subgrid constant is not yet available at this stage, all the models are considered through their basic representation, which is founded on a subgrid scale coefficient deduced from the knowledge of only the Kolmogorov constant [Lilly’s value<sup>20</sup> for the Smagorinsky model; see Bardina *et al.* (1980)<sup>24</sup> and Meneveau and Katz (1996)<sup>25</sup> for the mixed model and Appendix A for the present model]. In this way it has been attempted to free the analysis from the peculiarities of the optimization process, which is always based on empirical information, which, if not known well and reproduced, could spoil the mutual comparisons of the models. Our analysis is mostly carried out using the very basic values of the subgrid coefficients, with a few supplements of information relevant to the Smagorinsky and mixed models—utilized with optimized coefficients<sup>25</sup>—to be introduced into the comparative analysis, where opportune. On the other hand, to escape from the complexity linked to the introduction of a further step in the modeling process, we will also avoid comparing the models in the version that arises from the implementation of the dynamical procedure,<sup>26</sup> which, nevertheless, could always be adopted to substantially improve the performance of all the subgrid models (see the review by Meneveau and Katz, 2000).<sup>25</sup> The angular momentum subgrid model could, of course, undergo the dynamical procedure as could any other subgrid scale model.

The homogeneous and isotropic field used as the initial condition for all the large eddy simulations carried out to validate the present model is the 512<sup>3</sup> DNS database by Wray.<sup>27</sup> The initial distribution of the volume-averaged velocities and intrinsic moment of momenta are determined by averaging Wray’s data over cubes with  $2\delta$  sides corresponding to a LES spatial resolution of 64<sup>3</sup> points.

The energy temporal decays of homogeneous and isotropic turbulence, obtained from pseudospectral Navier–Stokes simulations over 64<sup>3</sup> points, implementing the angular momentum, the Smagorinsky and the mixed models, are shown in Fig. 1(a), together with the decay produced by the direct numerical simulation by Wray<sup>27</sup> over 512<sup>3</sup> points.

To make the LES temporal decays, obtained after filtering the DNS data, and the DNS decay comparable, the last decay is also shown after having applied at each instant a low-pass filter on the spectral energy that consists of the integration of the three-dimensional energy spectrum—included in the database at different eddy turnover times—over the lowest 32 wave numbers, which is equivalent to a spatial resolution of 64<sup>3</sup> points for the large eddy simulations.

The angular momentum model behaves well, since it performs slightly better than the basic Smagorinsky and the mixed models. The performances become equivalent if the

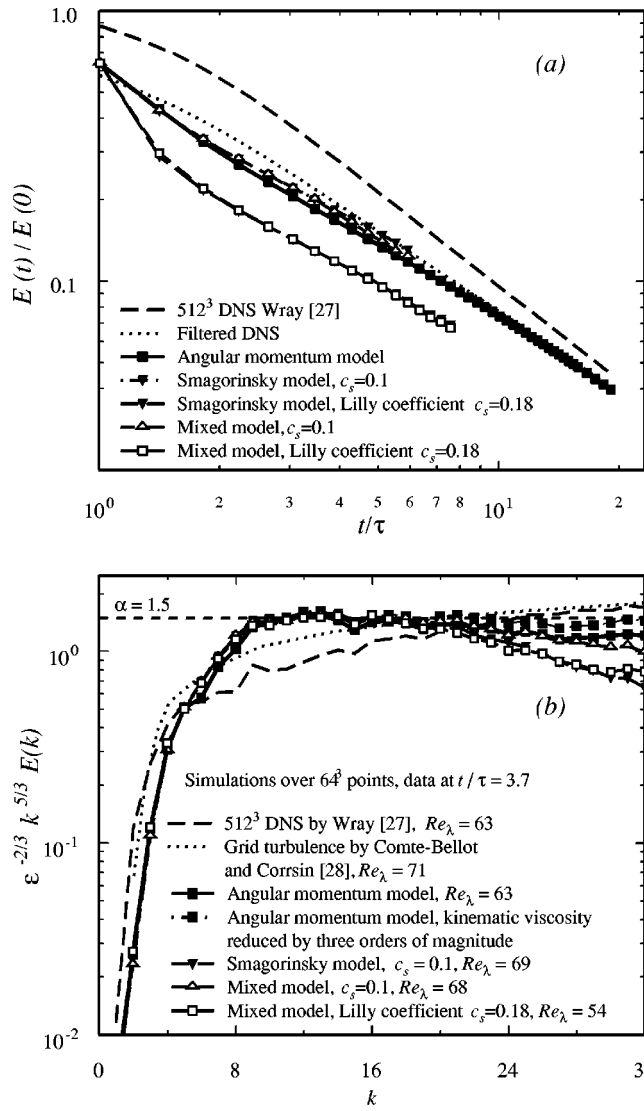


FIG. 1. Homogeneous isotropic turbulence: (a) turbulent kinetic energy decay; (b) compensated three-dimensional energy spectra at  $t/\tau = 3.7$ . For all the simulations, the initial condition of the velocity field is taken from Wray (Ref. 27).

Smagorinsky and the mixed models use their optimized subgrid constants. Figure 1(b) shows the compensated energy spectra, at  $t/\tau = 3.7$  and  $Re_\lambda \sim 65$ , as established through the experiments by Comte-Bellot and Corrsin,<sup>28</sup> the direct numerical simulation by Wray and through large eddy simulations based on the angular momentum model and the Smagorinsky and mixed subgrid models. In these diagrams the presence of a horizontal asymptote means the inertial range is reached. In this regard it can be seen that the basic (nonoptimized) angular momentum model results to be slightly more accurate than the other two models, even if used with their optimized subgrid coefficients.

A result concerning the energy transfer that characterizes a decaying homogeneous turbulent field under solid body rotation is presented for validation purposes in an anisotropy situation. Figure 2 presents the dependence of the velocity derivative skewness  $S$ , a quantity linked to the enstrophy production, on the inverse of the instantaneous micro-Rossby

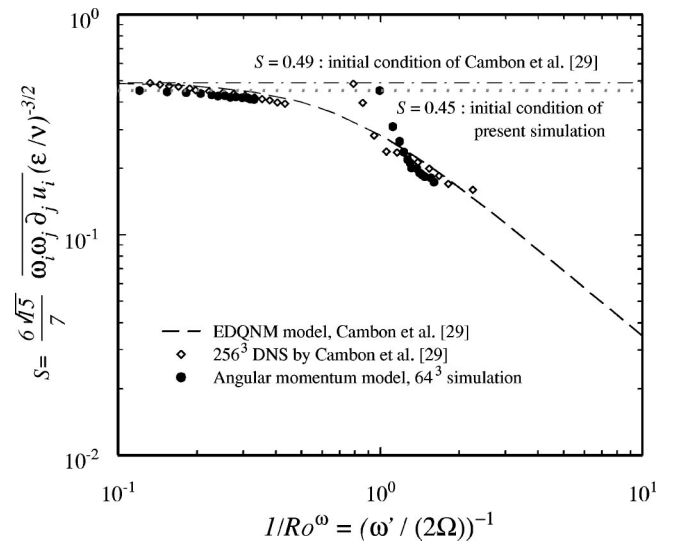


FIG. 2. Homogeneous turbulence undergoing a solid body rotation with angular speed  $\Omega$ . Velocity derivative skewness as a function of the inverse of the micro-Rossby number. For the angular momentum model simulations, the initial condition is taken from Wray (Ref. 27) and the computed points—black filled circles—are regularly spaced in time by 0.41 eddy turnover times. The ensemble average that defines the velocity derivative skewness  $S$  is approximated through the volume average over the whole computational domain.

number  $Ro_\omega = \overline{\omega'}/2\Omega$ , where  $\overline{\omega'}$  is the root mean square value of the vorticity and  $\Omega$  is the background vorticity. The two angular momentum large eddy simulations performed at initial micro-Rossby numbers greater than and nearly equal to 1 show a very good agreement with two different sets of data: the analytical representation of the evolution  $S = S(Ro_\omega)$  deduced from the collapse over a unique curve of many runs—with different initial  $Ro_\omega$  and a suddenly imposed rotation—of the basic EDQNM (eddy damped quasi-normal Markovian) model [see Cambon *et al.* (1997),<sup>29</sup> Fig. 3 and formula (3.5)] and two direct numerical computations at initial micro-Rossby numbers close to the ones we tested.

The angular momentum large eddy simulations in this case rely on a modified version of the averaged equations (14) and (15) written in a rotating frame of reference (in the absence of external forces and with centrifugal terms associated to the pressure gradient):

$$D_t \langle u_i \rangle + 2\epsilon_{i/k} \Omega_\ell \langle u_k \rangle = \rho^{-1} \partial_j \sigma_{kj} + \partial_j \tau_{ij}, \quad (23)$$

$$D_t h_i + 2\epsilon_{i/k} \epsilon_{kmn} \Omega_m (\langle x_\ell u_n \rangle - \langle x_\ell \rangle \langle u_n \rangle) = \rho^{-1} \partial_j s_{ij} + \partial_j c_{ij}, \quad (24)$$

where  $\Omega_\ell$  is the background constant angular rotation and the second term on the left-hand side of (24) is approximated—through a development in series of  $\delta$  of  $u_n$ —by

$$r_i \approx \frac{2}{3} \epsilon_{i/k} \epsilon_{kmn} \Omega_m \partial_\ell \langle u_n \rangle \delta^2.$$

This expression can be simplified, using Ricci's formulas ( $\epsilon_{i/k} \epsilon_{kmn} = \delta_{im} \delta_{ln} - \delta_{in} \delta_{lm}$ ) and the incompressibility constraint, to

$$r_i \approx -\frac{2}{3} \Omega \partial_j \langle u_i \rangle \delta^2.$$

This Coriolis angular momentum and the corresponding Coriolis force, the second term on the left-hand side of (23), are independent of the actual location of the axis of rotation and set the occurrence of a uniform background vorticity of value  $2\Omega$  on the flow, at a given initial time. During the next temporal decay of an initially isotropic and homogeneous turbulence, the background vorticity resists and prevents the twisting and stretching mechanism caused by the turbulence itself, which leads to a decrease of the decay rate of the turbulent kinetic energy. This phenomenology characterizes the numerical simulations of Fig. 2, where a much faster decay (together with an initial conservation of the properties of isotropy and three-dimensionality<sup>29,30</sup>) of the velocity derivative skewness corresponds to simulations with a lower initial Rossby number.

For the right-hand sides of (23) and (24) reference is made to Sec. III B.

The last validation result we present corresponds to a nonhomogeneous situation. The considered flow is the shearless mixing layer between two homogeneous and isotropic turbulences that have different kinetic energies. Also in this case, the angular momentum model performs very well, thus confirming the good spectral and correlation properties demonstrated in the preceding two examples. In particular, it can be noticed that its accuracy is higher than that of the basic Smagorinsky model ( $c_s=0.18$ ) and it is equivalent to that of the optimized Smagorinsky model ( $c_s=0.10$ ), even though it has not yet experienced an optimization process and its subgrid coefficient is based on the one and only piece of knowledge of the Kolmogorov constant. Figure 3 shows the profiles of the turbulent kinetic energy and velocity skewness of the mixing. The profile that gives a better indication of the prediction capability of the mixing dynamics is the skewness profile: the parameters that show a good intermittency behavior are the value and the position of the maximum of the skewness. The angular momentum simulations yield a velocity skewness profile that compares very well with the direct numerical simulation by Briggs *et al.* (1996)<sup>31</sup> and the experiment by Veeravalli and Warhaft (1989)<sup>32</sup> and that compares in the previously described way with regards to the Smagorinsky model.<sup>18</sup> This set of simulations is based on initial homogeneous and isotropic turbulent fields by Wray<sup>27</sup> and Orlandi.<sup>33</sup>

All the presented large eddy simulations were obtained by means of a new dealiased pseudospectral Fourier–Galerkin Navier–Stokes code (see Iovieno *et al.*<sup>34</sup>), implementing a fourth-order explicit Runge–Kutta scheme in the low storage version by Jameson *et al.* (1981).<sup>35</sup>

#### IV. CONCLUSIONS

By means of a series expansion in terms of  $\delta^2 - \delta$  being the linear dimension of the average—a new representation of the averaged angular momentum balance has been determined in terms of an infinite sequence of independent differential equations where linear antisymmetric operators act on the momentum. The first term of the sequence is the Helm-

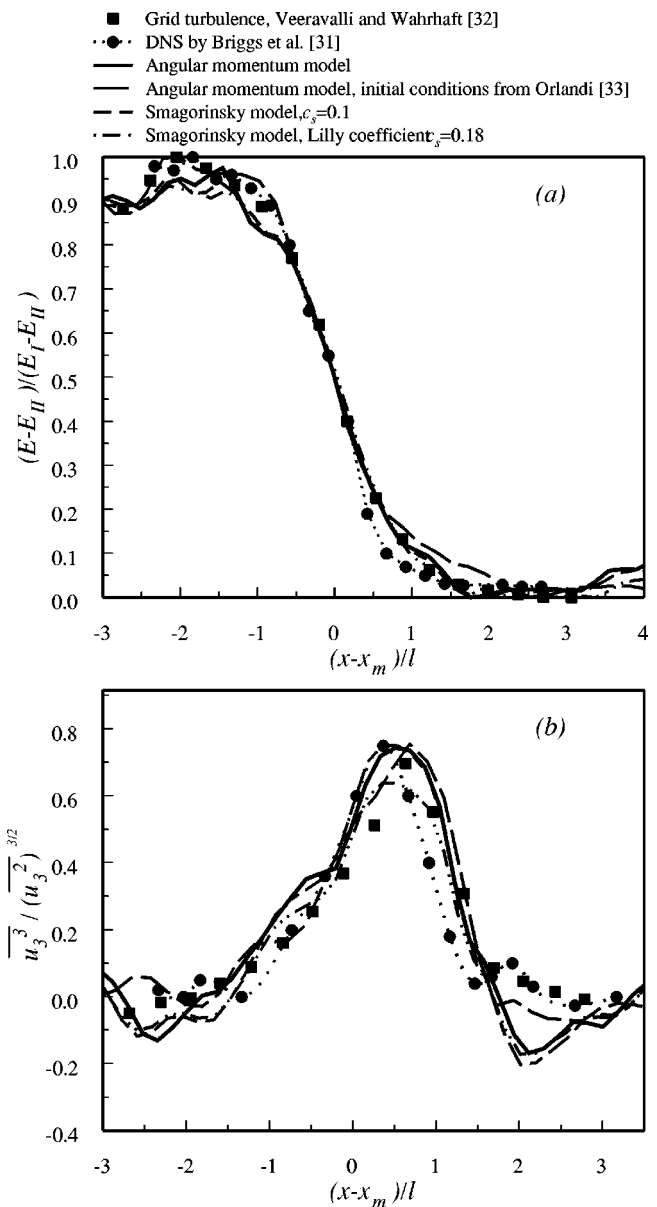


FIG. 3. Shear-free decaying turbulent mixing ( $t/\tau=5.35$ ): (a) profile of the nondimensional turbulent kinetic energy; (b) profile of the velocity skewness. Whenever not differently specified, the initial condition for the large eddy simulations is taken from Wray (Ref. 27). The ensemble averages defining the velocity skewness are approximated through the computation of mean values over surfaces normal to the non homogeneity direction.

holtz equation. The others may be viewed as kinds of high-order vorticity equations and could be used in turbulence mechanics as auxiliary equations to describe the evolution of the correlation variables obtained from the filtering of the turbulent equations. This representation could also be applied to the motion of structured fluid, as long as they can be considered as locally homogeneous.

The spatial filtering is not able to introduce asymmetries into homogeneous flows, even though they are in turbulent motion. The application of models suited to flows of a structured fluid and characterized by the coupling of the momentum and angular momentum equations, through the presence of an antisymmetric part of the stress tensor, to turbulent flows is not justified in our opinion.



A new differential large eddy scale model has been proposed that is based on a different kind of coupling of the momentum and angular momentum equations and that relies on the assumption of a turbulent diffusivity that is proportional to the intrinsic moment of momentum. This coupling does not spoil the symmetry property of the stress tensor. The model shows a proper scaling of the eddy diffusivity with respect either to the filtering length or the dissipation function and thus to the integral scale of the motion and it contains only one subgrid scale coefficient. In the case of turbulent motion of a structured fluid, where the coupling is already present, owing to the physical nature of the problem, the model becomes algebraic.

The model performs in a very positive way. The process of validation was based on a comparative analysis carried out on statistical and spectral results pertinent to homogeneous isotropic and nonisotropic turbulent flows, as well as to a nonhomogenous example. The compared reference results have been obtained from laboratory experiments, direct numerical simulations, and large eddy simulations relevant to three kinds of subgrid models, namely the Smagorinsky, the mixed, and the statistical EDQNM models.

## ACKNOWLEDGMENTS

The authors would like to thank Professor C. Cancelli, Professor C. Cercignani, Professor M. Germano, and Professor P. Orlandi for their useful suggestions.

## APPENDIX A: EVALUATION OF THE MODEL CONSTANT

In this section, the constant  $c$  of the model, defined by Eq. (19) of Sec. III B, is estimated assuming that the largest resolvable wave number  $2\pi/\delta$  lies within the inertial range, that the energy transfer rate from the resolved scales to the subgrid scales is equal to the energy dissipation rate  $\varepsilon$  and that a great separation of scales exists. In such a situation the energy of the subgrid scales is mostly that of their inertial part. Under this assumption, Yoshizawa<sup>21</sup> determined the constant of the scaling law for the eddy viscosity,

$$\nu_\delta = c_\nu \varepsilon^{4/3} \delta^{1/3}, \quad c_\nu \approx 0.053.$$

Considering spherical average volumes, of radius  $\delta$ , it is possible to write the intrinsic angular momentum  $h$ , introduced into Sec. II, as

$$h \approx \frac{3}{4\pi\delta^3} \int_0^\delta u_\lambda 4\pi\lambda^3 d\lambda, \quad (\text{A1})$$

where  $u_\lambda$  is the turbulent velocity variation over distances of the order  $\lambda$ . The Kolmogorov's law yields

$$u_\lambda = (3\alpha)^{1/2} \left( \frac{\varepsilon\lambda}{2\pi} \right)^{1/3},$$

where  $\alpha$  is the Kolmogorov constant, which is approximately equal<sup>20</sup> to 1.5. Integral (A1) therefore leads to

$$h = c_h \varepsilon^{4/3} \delta^{1/3}, \quad c_h = \frac{9(3\alpha)^{1/2}}{13(2\pi)^{1/3}} \approx 0.80,$$

and the constant  $c$  in (19) is consequently

$$c = \frac{c_\nu}{c_h} \approx 0.066,$$

a value that has been successfully confirmed through the validation process described in Sec. III C [also see Iovieno (2001)<sup>36</sup>].

## APPENDIX B: COMPARATIVE ANALYSIS BETWEEN THE MIXED AND THE ANGULAR MOMENTUM MODELS

Let us consider the spatial average  $\langle f \rangle_\delta$  introduced into Sec. II [Eq. (1)]. In analogy with what has already been done for the operator  $\mathbf{M}$  [see Eqs. (3)–(6)] expanding  $f$  in the neighborhood of  $\mathbf{x}$  and introducing the transformation  $\boldsymbol{\eta} = \delta\boldsymbol{\zeta}$ , we obtain

$$\begin{aligned} \langle f \rangle &= \sum_{m=0}^{\infty} \sum_{j=0}^m \sum_{i=0}^j \frac{\delta^{2m}}{(2m)!} \binom{2m}{2j} \binom{2j}{2i} \\ &\times \left( \frac{1}{V_1} \int_{\mathcal{I}_1} \zeta_1^{2(m-j)} \zeta_2^{2(j-i)} \zeta_3^{2i} d\boldsymbol{\zeta} \right) \partial_1^{m-j} \partial_2^{j-i} \partial_3^i f(\mathbf{x}). \quad (\text{B1}) \end{aligned}$$

The symmetry property of  $\mathcal{I}_\delta$  had to be used to obtain relation (B1). As a consequence, the coefficients of the expansion contain integrals whose kernels are the product of even powers of the components of the space variable  $\boldsymbol{\zeta}$ . These normalized integrals can be written in the form

$$\frac{1}{V_1} \int_{\mathcal{I}_1} \zeta_\ell^{2\alpha} \zeta_p^{2\beta} \zeta_q^{2\gamma} d\boldsymbol{\zeta} = c^{\alpha,\beta,\gamma}, \quad (\text{B2})$$

where  $\alpha, \beta, \gamma \in \mathbb{N}$  and  $\ell, p, q$  is any permutation of 1, 2, and 3. Notice that the same is also true for the coefficients  $a^{n,m,\ell}$  of the intrinsic angular momentum expansion [see Sec. II (5)]. The general coefficient  $c^{\alpha,\beta,\gamma}$  can therefore be introduced into both expansions (6) and (B1).

Let us now consider the truncated fourth-order  $\delta$  expansion for  $\langle f \rangle$ :

$$\begin{aligned} \langle f \rangle(\mathbf{x}) &= f(\mathbf{x}) + \frac{1}{2} c^{1,0,0} \nabla^2 f(\mathbf{x}) \delta^2 \\ &+ \frac{1}{4!} [c^{2,0,0} (\partial_\ell^4 + \partial_p^4 + \partial_q^4) f(\mathbf{x}) \\ &+ 6c^{1,1,0} (\partial_\ell^2 \partial_p^2 + \partial_\ell^2 \partial_q^2 + \partial_p^2 \partial_q^2) f(\mathbf{x})] \delta^4 + O(\delta^6) \\ &= f(\mathbf{x}) + F^{(1)}[f] \delta^2 + F^{(2)}[f] \delta^4 + O(\delta^6). \quad (\text{B3}) \end{aligned}$$

To highlight the partial analogy, presented in Sec. III B, that links the angular momentum and the mixed models, we need to compare, on one hand, the expansions in powers of  $\delta^2$  of the subgrid turbulent momentum stress  $\tau_{ij}$  and of the similarity term of the mixed model  $\tau_{ij}^{\text{sim}}$  and, on the other hand, the expansions of the subgrid angular momentum stress (16) and of the stretching term  $\langle u_i \rangle h_j$  of its model (21). The use of (B3) to approximate  $\langle u_i \rangle$  and  $\langle u_i u_j \rangle$  and of expansion (8), rewritten in terms of coefficients (B2), to approximate  $h_i$ , yields the following expansion of the order  $\delta^4$ .

(i) *Subgrid turbulent momentum stress:*

$$\begin{aligned} \tau_{ij} &= \langle u_i \rangle \langle u_j \rangle - \langle u_i u_j \rangle \\ &= (u_i + F^{(1)}[u_i])\delta^2 + F^{(2)}[u_i]\delta^4 + O(\delta^6) \\ &\quad \times (u_j + F^{(1)}[u_j]\delta^2 + F^{(2)}[u_j]\delta^4 + O(\delta^6)) \\ &\quad - (u_i u_j + F^{(1)}[u_i u_j]\delta^2 + F^{(2)}[u_i u_j]\delta^4 + O(\delta^6)) \\ &= (u_i F^{(1)}[u_j] + u_j F^{(1)}[u_i] - F^{(1)}[u_i u_j])\delta^2 \\ &\quad + (u_i F^{(2)}[u_j] + u_j F^{(2)}[u_i] + F^{(1)}[u_i]F^{(1)}[u_j] \\ &\quad - F^{(2)}[u_i u_j])\delta^4 + O(\delta^6). \end{aligned} \tag{B4}$$

(ii) *Similarity term of the mixed model.* Replacing  $u_i$  ed  $u_j$  with  $\langle u_i \rangle$  ed  $\langle u_j \rangle$  in the previous result,

$$\begin{aligned} \tau_{ij}^{\text{sim}} &= \langle \langle u_i \rangle \rangle \langle \langle u_j \rangle \rangle - \langle \langle u_i u_j \rangle \rangle \\ &= (\langle u_i \rangle F^{(1)}[\langle u_j \rangle] + \langle u_j \rangle F^{(1)}[\langle u_i \rangle] \\ &\quad - F^{(1)}[\langle u_i u_j \rangle])\delta^2 + (\langle u_i \rangle F^{(2)}[\langle u_j \rangle] \\ &\quad + \langle u_j \rangle F^{(2)}[\langle u_i \rangle] + F^{(1)}[\langle u_i \rangle]F^{(1)}[\langle u_j \rangle] \\ &\quad - F^{(2)}[\langle u_i \rangle \langle u_j \rangle])\delta^4 + O(\delta^6) \end{aligned}$$

and introducing  $\langle u_i \rangle = u_i + F^{(1)}[u_i] + O(\delta^4)$  and  $\langle u_j \rangle = u_j + F^{(1)}[u_j] + O(\delta^4)$ ,

$$\begin{aligned} \tau_{ij}^{\text{sim}} &= (u_i F^{(1)}[u_j] + u_j F^{(1)}[u_i] - F^{(1)}[u_i u_j])\delta^2 \\ &\quad + (u_i F^{(2)}[u_j] + u_j F^{(2)}[u_i] + F^{(1)}[u_i]F^{(1)}[u_j] \\ &\quad - F^{(2)}[u_i u_j] + u_i F^{(1)}[F^{(1)}[u_j]] + u_j F^{(1)}[F^{(1)}[u_i]]) \\ &\quad + 2F^{(1)}[u_i]F^{(1)}[u_j] - F^{(1)}[F^{(1)}[u_i u_j]]\delta^4 \\ &\quad + O(\delta^6). \end{aligned} \tag{B5}$$

(iii) *Subgrid turbulent angular momentum stress:*

$$\begin{aligned} c_{ij} &= \varepsilon_{i\ell k} [(\langle x_\ell u_k \rangle - \langle x_\ell \rangle \langle u_k \rangle) \langle u_j \rangle - (\langle x_\ell u_k u_j \rangle \\ &\quad - \langle x_\ell \rangle \langle u_k u_j \rangle)]. \end{aligned}$$

First, expanding

$$\begin{aligned} \langle x_\ell u_k \rangle - \langle x_\ell \rangle \langle u_k \rangle &= c^{1,0,0} \partial_\ell u_k \delta^2 + \frac{1}{3!} [(c^{2,0,0} - 3c^{1,1,0}) \\ &\quad \times \partial_\ell^3 u_k + 3c^{1,1,0} \partial_\ell \nabla^2 u_k] \delta^4 + O(\delta^6), \end{aligned}$$

then introducing  $\langle u_i \rangle = u_i + \delta^2 F^{(1)}[u_i] + O(\delta^4) = u_i + \frac{1}{2} c^{1,0,0} \delta^2 \nabla^2 u_i + O(\delta^4)$  yields

$$\begin{aligned} (\langle x_\ell u_k \rangle - \langle x_\ell \rangle \langle u_k \rangle) \langle u_j \rangle &= c^{1,0,0} u_j \partial_\ell u_k \delta^2 + \left( \frac{u_j}{3!} [(c^{2,0,0} - 3c^{1,1,0}) \partial_\ell^3 u_k \right. \\ &\quad \left. + 3c^{1,1,0} \partial_\ell \nabla^2 u_k] + \frac{1}{2} (c^{1,0,0})^2 \partial_\ell u_k \nabla^2 u_j \right) + O(\delta^6), \end{aligned}$$

while

$$\begin{aligned} \langle x_\ell u_k u_j \rangle - \langle x_\ell \rangle \langle u_k u_j \rangle &= c^{1,0,0} \partial_\ell (u_k u_j) \delta^2 + \frac{1}{3!} [(c^{2,0,0} - 3c^{1,1,0}) \partial_\ell^3 (u_k u_j) \\ &\quad + 3c^{1,1,0} \partial_\ell \nabla^2 (u_k u_j)] \delta^4 + O(\delta^6). \end{aligned}$$

One eventually obtains

$$\begin{aligned} c_{ij} &= c^{1,0,0} u_i \omega_j \delta^2 + \varepsilon_{i\ell k} \left( \frac{u_j}{3!} [(c^{2,0,0} - 3c^{1,1,0}) \partial_\ell^3 u_k \right. \\ &\quad \left. + 3c^{1,1,0} \partial_\ell \nabla^2 u_k] + \frac{1}{2} (c^{1,0,0})^2 \partial_\ell u_k \nabla^2 u_j \right. \\ &\quad \left. - \frac{1}{3!} [(c^{2,0,0} - 3c^{1,1,0}) \partial_\ell^3 (u_k u_j) \right. \\ &\quad \left. + 3c^{1,1,0} \partial_\ell \nabla^2 (u_k u_j)] \right) \delta^4 + O(\delta^6). \end{aligned} \tag{B6}$$

(iv) *Stretching part of model (21) for  $c_{ij}$*

$$\begin{aligned} \langle u_i \rangle h_j &= [u_i + \frac{1}{2} c^{1,0,0} \nabla^2 u_i \delta^2 + O(\delta^4)] \\ &\quad \times \left( c^{1,0,0} \omega_j \delta^2 + \frac{1}{3!} [3c^{1,1,0} \nabla^2 \omega_j \right. \\ &\quad \left. + (c^{2,0,0} - 3c^{1,1,0}) \varepsilon_{j\ell k} \partial_\ell^3 u_k] \delta^4 + O(\delta^6) \right) \\ &= c^{1,0,0} u_i \omega_j \delta^2 + \left( \frac{(c^{1,0,0})^2}{2} \omega_j \nabla^2 u_i \right. \\ &\quad \left. + \frac{u_i}{3!} [3c^{1,1,0} \nabla^2 \omega_j + (c^{2,0,0} \right. \\ &\quad \left. - 3c^{1,1,0}) \varepsilon_{j\ell k} \partial_\ell^3 u_k] \right) \delta^4 + O(\delta^6). \end{aligned} \tag{B7}$$

Comparing expansions (B3) and (B4) it can be seen that the terms of the order  $\delta^2$  are identical. An analysis of the difference of the fourth-order terms shows that it cannot be equal to zero. Carrying out all the possible simplifications, it, in fact, results that this difference is equal to the Laplacian of the coefficient of the  $\delta^2$  term plus the products between the gradient of the velocity and the gradient of the Laplacian of the velocity. An equivalent situation holds for (B5) and (B6), therefore the analogy under discussion can be inferred. The comparison of (B3) to (B4) and of (B5)–(B6) shows that, to the order  $\delta^2$ ,  $\tau_{ij} \approx \tau_{ij}^{\text{sim}}$ , as does  $c_{ij} \approx \langle u_i \rangle h_j$ .

<sup>1</sup>G. K. Batchelor, "The stress system in a suspension of free-force particles," *J. Fluid Mech.* **44**, 545 (1970).

<sup>2</sup>J. S. Dahler and L. E. Scriven, "Theory of structured continua: general consideration of angular momentum and polarization," *Proc. R. Soc. London, Ser. A* **275**, 504 (1963).

<sup>3</sup>D. W. Condiff and J. S. Dahler, "Fluid mechanical aspects of antisymmetric stress," *Phys. Fluids* **7**, 842 (1964).

<sup>4</sup>H. Brenner, "Rheology of two-phase systems," *Annu. Rev. Fluid Mech.* **2**, 137 (1970).

<sup>5</sup>Y. Almog and H. Brenner, "Ensemble-average versus suspension scale Cauchy continuum mechanical definition of stress in polarized suspensions: Global homogenization of a dilute suspension of dipolar spherical particles," *Phys. Fluids* **11**, 268 (1999).

<sup>6</sup>A. C. Eringen, "Micropolar fluids," *J. Math. Mech.* **16**, 1 (1966).

<sup>7</sup>M. Kafadar and A. C. Eringen, "Micropolar fluids: the classical theory," *Int. J. Eng. Sci.* **9**, 271 (1971).

<sup>8</sup>G. Lukaszewicz, *Micropolar Fluids* (Birkhäuser, Basel, 1999).

<sup>9</sup>G. D. Mattioli, "Sur la théorie de la turbulence dans les canaux," *C. R. Acad. Sci.* **196**, 1282 (1933).

<sup>10</sup>G. D. Mattioli, *Teoria Dinamica dei Regimi Fluidi Turbolenti* (Cedam, Padova, 1937).

- <sup>11</sup>V. N. Nikolaevsky, "Asymmetric mechanics of turbulent flows," *Appl. Math. Mech.* **34**, 514 (1970).
- <sup>12</sup>V. N. Nikolaevsky, "Asymmetric mechanics of turbulent flows: energy and entropy," *Appl. Math. Mech.* **37**, 94 (1973).
- <sup>13</sup>A. C. Eringen, "Micromorphic description of turbulent channel flow," *J. Math. Anal. Appl.* **39**, 253 (1972).
- <sup>14</sup>P. C. Chatwin, "The vorticity equation as an angular momentum equation," *Proc. Cambridge Philos. Soc.* **74**, 365 (1973).
- <sup>15</sup>R. N. Nigmatulin and V. N. Nikolaevsky, "Diffusion of vorticity and the balance of momentum of momentum in dynamics of nonpolar fluids," *Appl. Math. Mech.* **34**, 318 (1970).
- <sup>16</sup>C. Ferrari, "On the differential equations of turbulent flow," in *Continuum Mechanics and Related Problems of Analysis* (Acad. Sci. USSR, Moscow, 1972), pp. 555–566.
- <sup>17</sup>J. Laufer, "Investigation of turbulent flow in two-dimensional channel," NASA TR-1053, 1951.
- <sup>18</sup>J. Smagorinsky, "General circulation experiments with the primitive equations," *Mon. Weather Rev.* **91**, 99 (1963).
- <sup>19</sup>D. Kwak, W. C. Reynolds, and J. H. Ferziger, "Tree-dimensional time dependent computation of turbulent flow," Stanford University Report TR-5, 1975.
- <sup>20</sup>D. K. Lilly, "The representation of small-scale turbulence in numerical simulation experiments," *Proceedings of the IBM Scientific Symposium on Environmental Sciences*, 1967.
- <sup>21</sup>A. Yoshizawa, "A statistically derived subgrid model for the large eddy simulation of turbulence," *Phys. Fluids* **25**, 1532 (1982).
- <sup>22</sup>A. S. Yaglom and A. M. Monin, *Statistical Fluid Mechanics* (MIT Press, Cambridge, 1975), Vol. 2.
- <sup>23</sup>D. C. Leslie and G. L. Quarini, "The application of turbulence theory to the formulation of subgrid modelling procedures," *J. Fluid Mech.* **91**, 65 (1979).
- <sup>24</sup>J. Bardina, J. H. Ferziger, and W. C. Reynolds, "Improved subgrid-scale models for large-eddy simulation," AIAA Paper 80-1357, 1980.
- <sup>25</sup>C. Meneveau and J. Katz, "Scale invariance and turbulence models for large-eddy simulation," *Annu. Rev. Fluid Mech.* **32**, 1 (2000).
- <sup>26</sup>M. Germano, "Turbulence: the filtering approach," *J. Fluid Mech.* **238**, 325 (1992).
- <sup>27</sup>A. A. Wray, "Data sheets for homogeneous flows, HOM02," in AGARD-AR-345 A Selection of Test Cases for the Validation of Large-Eddy Simulations of Turbulent Flows, 1998, p. 63.
- <sup>28</sup>G. Comte-Bellot and S. Corrsin, "Simple Eulerian time correlation of full- and narrow-band velocity signals in grid-generated, isotropic turbulence," *J. Fluid Mech.* **48**, 273 (1971).
- <sup>29</sup>C. Cambon, N. N. Mansour, and F. S. Godeferd, "Energy transfer in rotating turbulence," *J. Fluid Mech.* **337**, 303 (1997).
- <sup>30</sup>N. Mansour, T. H. Shih, and W. C. Reynolds, "The effects of rotation on initially anisotropic homogeneous flows," *Phys. Fluids A* **3**, 2421 (1991).
- <sup>31</sup>D. A. Briggs, J. H. Ferziger, J. R. Koseff, and S. G. Monismith, "Entrainment in a shear-free turbulent mixing layer," *J. Fluid Mech.* **310**, 215 (1996).
- <sup>32</sup>S. Veeravalli and Z. Warhaft, "The shearless turbulence mixing layer," *J. Fluid Mech.* **207**, 191 (1989).
- <sup>33</sup>P. Orlandi, Università La Sapienza, personal collection of turbulent fields, Rome, June 2001.
- <sup>34</sup>M. Iovieno, C. Cavazzoni, and D. Tordella, "A new technique for a parallel dealiased pseudospectral Navier–Stokes code," *Comput. Phys. Commun.* **141**, 364 (2001).
- <sup>35</sup>E. Jameson, H. Schmidt, and E. Turkel, "Numerical solutions of the Euler equations by finite volume methods using Runge–Kutta stepping schemes," AIAA Paper 81-1259, 1981.
- <sup>36</sup>M. Iovieno, Tesi di dottorato, Politecnico di Torino, 2001.